10-21-1992

Calibration of Atomic Force Microscope Tips Using Biomolecules

T. Thundat
Oak Ridge National Laboratory

X.-Y. Zheng
Oak Ridge National Laboratory

S. L. Sharp
Oak Ridge National Laboratory

D. P. Allison
Oak Ridge National Laboratory

R. J. Warmack
University of Tennessee, Knoxville

See next page for additional authors

Calibration of Atomic Force Microscope Tips Using Biomolecules

Authors

T. Thundat, X.-Y. Zheng, S. L. Sharp, D. P. Allison, R. J. Warmack, D. C. Joy, and T. L. Ferrell

CALIBRATION OF ATOMIC FORCE MICROSCOPE TIPS USING BIOMOLECULES

T. Thundat[*], X.-Y. Zheng, S. L. Sharp, D. P. Allison,
R. J. Warmack[2], D. C. Joy[1,2], and T. L. Ferrell[2]

Health and Safety Research Division, Oak Ridge National Laboratory, Oak Ridge, TN 37831-6123,
[1]HTML, Oak Ridge National Laboratory, Oak Ridge, TN 37831
[2]also at University of Tennessee, Knoxville TN 37996

Abstract

Atomic force microscope (AFM) images of surfaces and samples mounted on substrates are subject to artifacts such as broadening of structures and ghost images of tips due to the finite size and shape of the contacting probe. Therefore, knowledge of the radius of the AFM probe tip is essential for the interpretation of images. We have deduced the shape of the AFM tip by imaging cylindrical biological molecules of various diameters such as deoxyribonucleic acid (DNA), tobacco mosaic virus (TMV), tobacco etch virus (TEV) and bacteriophage M-13 (M-13). Using a paraboloidal tip model and numerically solving equations of contact, the curvatures of the tip and lithographically sharpened tip were ascertained.

Key Words: Atomic force microscopy, virus, tip, deoxyribonucleic acid, bacteriophage, mathematical models.

*Address for correspondence:
Thomas Thundat
Oak Ridge National Laboratory
P.O. Box 2008, MS-6123
Oak Ridge, TN 37831-6123
                    Telephone number: (615) 574-6215
                         FAX number: (615) 574-6210

Introduction

The atomic force microscope (AFM), invented by Binnig (Binnig *et al.*, 1986), has proven to be a powerful tool for obtaining high resolution images on both conducting and insulating surfaces in air as well as in liquid environments. Images are obtained by recording the deflections of a cantilever as the sample is scanned underneath the cantilever tip (see for example, Sarid, 1991) and the measured deflections are proportional to the force between the tip and the surface. Recently, the AFM has been used successfully to obtain reproducible images of DNA on mica (Henderson 1992; Thundat *et al.*, 1992a, 1992b) and on chemically treated mica (Bustamante *et al.*, 1992; Hansma *et al.*, 1992; Vesenka *et al.*, 1992; Lindsay *et al.*, 1992; Thundat *et al.*, 1992c). These DNA images demonstrate the enormous potential of the AFM to make contributions in structural biology. However, the resolution of the AFM is limited by the sharpness and shape of the tip and interpretation of images requires an understanding of tip geometry. For example, due to the finite radius of the tip AFM images of DNA are on average 7 times broader than the known 2 nm width of DNA. This unwanted broadening makes observation of fine details of the sample's surface difficult and limits the role of the AFM for imaging biological molecules. The quality of AFM images of DNA will rival those obtained with the conventional electron microscope only after the development of sharper tips. Techniques to sharpen tips using contamination lithography have been reported (Keller and Chung, 1992; Hansma *et al.*, 1992) and fabrication techniques to make sharper tips using silicon are being pursued (Wolter *et al.*, 1991).

For both a better understanding of the broadening phenomena and the interpretation of images a detailed understanding of the geometry of the AFM tip is essential. Using both commercially available tips (Nanoprobes, Digital Instruments; Ultralevers, Park Instruments) and commercial tips sharpened by contamination lithography in our own laboratory we have imaged biological samples with known, highly-uniform dimensions. The biomolecules used, deoxyribonucleic acid (DNA), bacteriophage M-13 (M-13), tobacco etch virus (TEV),

and tobacco mosaic virus (TMV) form an ascending set of probes to measure the region of the AFM tip with a corresponding curvature. From the measured widths of biomolecules a model for the AFM tip can be empirically derived.
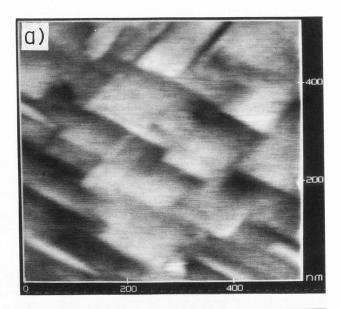
Materials and Methods

Plasmid DNA (pBS$^+$ from Stratagene, 3204 base pairs) at a concentration 20 μg/ml in 0.01 M ammonium acetate at pH 7.0 was used in this study (Allison *et al.*, 1992). The substrates for DNA were prepared by immersing freshly cleaved mica overnight in 10 mM solution of magnesium acetate or cobalt chloride, followed by a thorough rinsing in distilled water and ultrasonic cleaning in distilled water. The treated surfaces were heated at 105 °C for 48 hours before placing 100 μl of DNA solution onto the substrate for 1 minute and rinsing in a mixture of water and alcohol (1:1 ratio). The surface was air dried thoroughly before imaging in the AFM.

Virus and bacteriophage samples (TMV, TEV, and M-13) used in this study were prepared by allowing a 20 μl drop of the sample, at a concentration of 1-5 μg/ml in 0.01 M ammonium acetate pH 7.0, to air dry onto a freshly cleaved mica surface. The samples were dried in air and stored in a desiccator until used.

AFM studies were carried out on a commercially available Nanoscope II (Digital Instruments, Santa Barbara, CA). The commercial cantilevers used were 200 μm long microfabricated Si_3N_4 with a spring constant 0.12 N/m (Nanoprobes, Digital Instruments, Santa Barbara, CA). The homemade sharp tips used in this study were fabricated in our laboratory by contamination lithography using a scanning electron microscope (SEM). The tips were grown on the apex of commercially available (Nanoprobe) pyramidal tips in a Hitachi 800 SEM with a 5 nm spot size. We have also used commercially available sharp silicon tips that are 180 μm long with a spring constant of 0.008 N/m (Ultralevers, Park Inst., Sunnyvale, CA). All images were taken in air with a constant force of 1-3 nN and with an information density of 400 X 400 points and are presented as flattened raw data. Since the widths of the DNA images were found to be affected by relative humidity (Thundat *et al.*, 1992b), imaging was done at a relative humidity of less than 20% by placing the AFM in a humidity-controlled box purged with dry nitrogen.

Results and Discussion

The resolution of AFM images is greatly affected by the radius of the contacting probe. Figure 1 shows AFM (a) and STM (b) images of a platinum surface vapor deposited onto mica. The AFM images were obtained using commercial (Nanoprobe) tips where the half angle of the pyramidal tip is 36°. Therefore, the vertical drop of a step edge when contacted with the pyramidal tip will appear as a slope and much of the fine
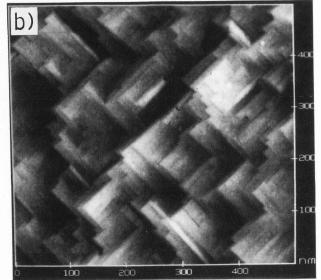

Figure 1. AFM (a) and STM (b) topograph of Pt on mica. Black (low) to white (high) represents 20 nm Z-height.

structure seen with the STM are lost in the AFM image. In extreme cases, where the surface topography of the sample contains dendritic features that are sharper than the tip, the image obtained will be an image of the tip (Fig. 2). Rotating the sample by 45° changes the position but not the orientation of these squares, but rotating the scan direction does change the orientation of the squares. This observation can be explained if we understand that in scanned probe microscopies the image obtained is a convolution of the tip curvature with the sample curvature. For greatly differing curvatures, the sharper object always images the blunter object irrespective of whether the sharper object is the tip or the sample. Therefore, the squares seen in the images are
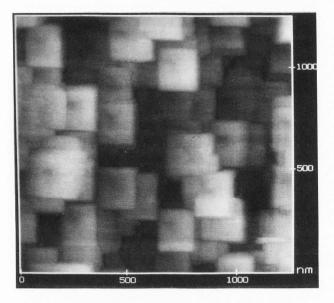
Figure 2. AFM image of gold surface (evaporated on mica) showing artifacts produced by tip. The squares are ghost images of the tip. Black (low) to white (high) corresponds to 700 nm.

----

predominantly the images of the AFM tip produced by dendrites on the gold surface. AFM images similar to those shown in Figure 2 (but at a lesser density) on a gold surface have also been reported (Oden *et al.*, 1992). We have occasionally found such tip images within images of diamond surfaces grown by chemical vapor deposition and within images of DNA adsorbed on mica probably caused by sharp salt crystallites dried on the surface.

Interpretation of AFM images of surfaces and of molecular adsorbates on surfaces depends both on understanding tip geometry (half angle, height, etc.) and knowing the curvature of the tip. Using cylindrical biological molecules of known dimensions we have derived a formula that can be used to accurately measure the contacting radius of AFM tips. DNA is a long cylindrical biomolecule with a diameter of 2 nm that can be imaged on chemically treated mica as shown in Figure 3. The average width of DNA strands measured from AFM images of circular pBS$^+$ was 14 nm. Sometimes it is possible to get images of DNA with a width of 9 nm possibly due to an accidentally sharpened tip. Recently, higher resolution images of DNA have been obtained using sharper tips in propanol (Hansma *et al.*, 1992). We also have observed that during the scan, the tip can pick up particles, possibly dried salt crystallites, to produce broader images.

Figures 4a and 4b show AFM images of the TMV dried on a freshly cleaved mica surface. The width and length of TMV are 18 nm and 300 nm, respectively (Matthews, 1981). The periodicity of closely packed TMV measured from a colony of TMV as shown in Figure 4a agrees with the accepted value and confirms the calibration of this AFM. The average height of TMV as
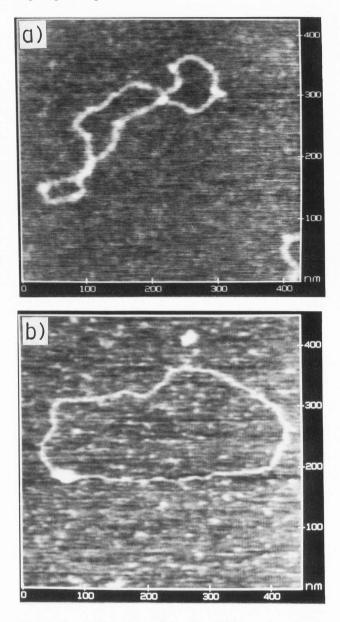

Figure 3. AFM images of circular DNA on mica chemically treated with Mg. Black (low) to white (high) corresponds to 10 nm. (a) taken with a normal tip and (b) imaged with a sharp tip. The average height of DNA measured from the image is 1.5 nm.

----

measured from AFM images is 17.8 nm. Recently, Li and Lindsay (1991) used latex spheres as a calibration standard for X, Y, and Z directions of AFM and found the periodicities of packed latex spheres to agree with the values given by the manufacturer. We observed that the individual strands of TMV (indicated by arrows) are wider than the strands inside the aggregate due to broadening by the tip (Fig. 4b). Similar observations of particles that aggregate, such as latex spheres and colloidal gold, also show images of wider particles at the edges of monolayer aggregates. The width of an isolated TMV is 48 nm while the average measured width (periodicity) of
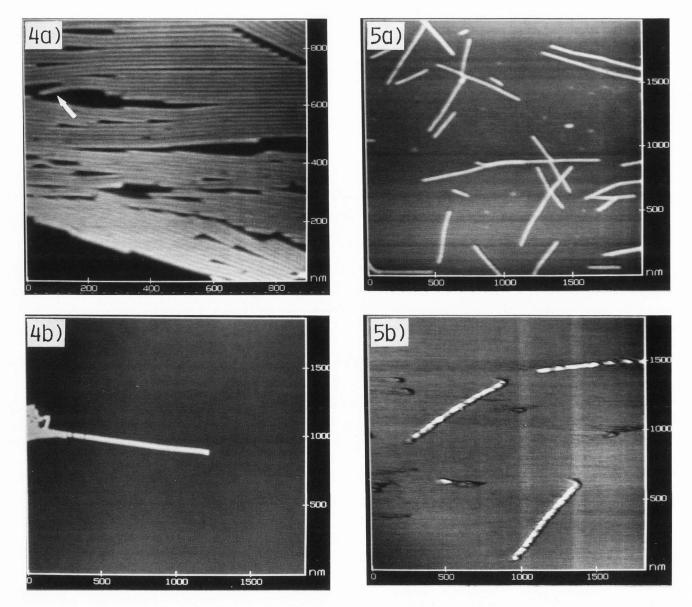
Figure 4. AFM images of tobacco mosaic virus (TMV). **(a)** TMV aggregate. The arrow points to broader strands. **(b)** An isolated strand sticking out of an aggregate.

Figure 5. AFM images of **(a)** M-13 bacteriophage and **(b)** tobacco etch virus on freshly cleaved mica. The average measured heights of M-13 and TEV are 5.4 nm and 8.3 nm, respectively.

---

molecules in the aggregate is 16 nm. Figure 5 shows AFM images of M-13 bacteriophage (a) and tobacco etch virus (b) on freshly cleaved mica. The known width of M-13 is 7 nm (Newberger and Tatum, 1975)) while the measured width of molecules from Figure 5a is 28 nm. The average height of M-13 measured from AFM image is 5.4 nm. Similarly the known width of TEV is 12 nm (Matthews, 1981) while the measured width from the AFM images of Figure 5b is 40 nm. The average height of TEV measured from AFM image is 8.3 nm. Unlike

TMV these molecules do not form aggregates on mica surfaces and it is relatively easy to find isolated molecules.

The increased width of isolated biomolecules observed in an AFM image is due to the geometrical interaction of the AFM tip profile with the sample geometry. The value of tip radius reported in the literature varies from 30 nm to 50 nm (Albrecht *et al.*, 1990; Keller and Chung, 1992). A simple geometrical model in which the tip is assumed to be a sphere of radius R and the biomolecule to be a sphere (or cylinder) of radius r

Figure 6. Geometrical representation (cross-section) of tip contacting the sample drawn to scale assuming a paraboloidal tip of radius 11 nm and different biomolecules used. The origin (0,0) is at the center of the sample (circle).

Table 1: Widths of the biomolecules used to probe the AFM tip. The calculated width is obtained from a paraboloidal tip model or a circular tip model (see the text for details).

Sample	Widths in nm			
	Accepted	Measured[1]	Calculated circular tip[2]	paraboloidal tip[3]
DNA	2	14.0 ± 1.9	14	14
M-13	7	27.9 ± 2.2	26	28
TEV	12	40.2 ± 2.5	34	39
TMV	18	48.3 ± 3.1	42	50

[1]The width is the average value of 10 measurements carried out at low humidity conditions.
[2]Tip radius used was 12.3 nm. This value was calculated from apparent width of DNA obtained by commercially available tips (Nanoprobes).
[3]The average value of $b = 0.046$ nm^{-1} was used in these calculations. This corresponds to a radius of curvature $(1/2b)$ at the tip of 10.9 nm.

----

causes an apparent width of $4(Rr)^{1/2}$. This calculation suggests that the tip radius will be a limiting factor in obtaining high resolution images of biomolecules assuming the tip and sample to be rigid. The radius of curvature of the tip calculated from the above equation using the measured dimensions of DNA in actual images is around 12.3 nm. Although this simple equation may provide excellent results for some molecules such as DNA, it breaks down for many larger molecules due to the deviation of the AFM tip from a spherical geometry (see Table 1). The point of contact of the molecules with the tip varies with the molecule probing different parts along the tip surface as shown in Figure 6.

A higher-order model considers the tip to be modeled as a paraboloid of revolution and the sample to be treated as a cylinder. Since our samples are on a flat surface, we need consider only the cross-section as shown in Figure 6. Here, the tip and sample are represented by a parabola and a circle, respectively, by the following expressions:

$$y = b\,(x - c)^2 + d \qquad (1)$$

$$x^2 + y^2 = a^2 \qquad (2)$$

where b is a parameter for the parabola and a is the radius of the sample. The apex of the tip position is denoted by (c,d). Since the origin $(0,0)$ is at the center of the circle (sample), $d = -a$ until the tip makes the initial contact with the sample and gives an apparent measured width $2c$. At the contact point, the tangents of the two curves are equal which gives:

$$c = (x/2by) + x \qquad (3)$$

Equations (1)-(3) can be solved numerically. For known values of a and c, we can determine the parameter b for the tip. We found, for the samples we measured, the average value of b to be 0.046 nm^{-1}. The radius of curvature at the apex of the paraboloid is given by $1/2b$, that gives a minimum radius of curvature of 10.9 nm for Nanoprobe tips that is much smaller than the 50 nm average value given in the literature. When the equation is applied to Ultralever tips we get a calculated value of 9 nm that agrees with the 10 nm tip radius given by the manufacturer. We can also solve the inverse problem, that is, with known b and c, we can determine the radius of the sample (assuming the compressibility of the sample is negligible). As shown in Table 1, the widths calculated from a paraboloidal tip model are in closer agreement with measured widths of the samples than widths calculated from a circular tip model.

We have also imaged DNA, TMV, TEV, and M-13 using tips sharpened by contamination lithography in

an SEM and found the apparent widths of biomolecules to be less than those obtained with commercial tips. Using the same analysis as above, the radii of contamination sharpened tips were calculated to be 9 nm. The limiting feature in micro-tip fabrication using contamination lithography appears to be the beam spot size. However, besides reducing the tip radius, the tip sharpening technique also appears to be better in avoiding artifacts such as ghost images and edge effects. A sharper tip with a high aspect ratio also reduces the capillary force due to the liquid bridge formed between the tip and the surface. The capillary forces (force required to break the cantilever away from the surface) measured from force curves were found to decrease by a factor of two or better when sharp micro-tips were used. Decreasing the capillary force decreases the effective area of contact which in turn improves the resolution. Figure 7a shows an AFM image of atomic steps on a gold surface imaged with a sharp tip produced by contamination lithography. When normal tips are used, the images fail to show atomic steps. Figure 7b and 7c show images of gold surfaces (evaporated on mica) imaged with sharp tip and a normal tip, respectively, at 50% relative humidity. More details can be seen on the gold surface with a sharper tip than with a regular tip. Although the details as shown in Figure 7b can be obtained with a normal tip by decreasing the size of the liquid bridge by decreasing humidity to very low values, the normal tips fail to image atomic steps.

Conclusion

We have deduced the shape of the AFM tip by imaging several cylindrical biological molecules (DNA, TMV, TEV, and M-13). The tip was approximated as a paraboloid and the cylindrical sample as a circle in cross-section. By solving the equations of contact numerically, it is possible to obtain tip parameters. The radii of curvature of commercially available Nanoprobes and Ultralever AFM tips were found to be approximately 11 nm and 9 nm, respectively. The radius of curvature of the tips produced in an SEM by contamination lithography was found to be 9 nm. Because of the higher aspect ratio of contamination sharpened tips, atomic steps can be easily found on gold surfaces. The capillary forces due to the liquid bridge formed between the tip and sample can be reduced by a factor of two or better by using contamination sharpened tips in normal humidity conditions (40-50%).

Acknowledgments

References

Albrecht TR, Akamine S, Craver TE, Quate CF (1990) Microfabrication of cantilever styli for atomic force microscope. J. Vac. Sci. Technol. **A8**: 3386-3396.

Allison DP, Warmack RJ, Bottomley LA, Thundat T, Brown GM, Woychik RP, Schrick JJ, Jacobson KB, Ferrell TL (1992) Scanning tunneling microscopy of DNA: A novel technique using radio labelled dna to evaluate chemically mediated attachment of DNA to surfaces. Ultramicrosc. **42-44**: 1088-1094.

Binnig G, Quate CF, Gerber Ch (1986) Atomic force microscope. Phys. Rev. Lett. **56**: 930-933.

Bustamante C, Vesenka J, Tang CL, Rees W, Guthold M, Keller R (1992) Circular DNA molecules imaged in air by scanning force microscopy. Biochem. **31**: 22-26.

Hansma HG, Vesenka J, Siegerist C, Kelderman G, Morrett H, Sinsheimer RL, Elings V, Bustamante C, Hansma PK (1992) Reproducible imaging and dissection of plasmid DNA under liquid with the atomic force microscope. Science **256**: 1180-1184.

Henderson E (1992) Imaging and nanodissection of individual super coiled plasmids by AFM. Nucleic Acid Res. **20**: 445-447.

Keller D, Chung CH (1992) Imaging steep, high structures by scanning force microscopy with electron beam deposited tips. Surf. Sci. **268**: 333-339.

Li Y, Lindsay SM (1991) Polystyrene Latex particles as a size calibration for the atomic force microscope. Rev. Sci. Instrum. **62**: 2630-2633.

Lindsay SM, Lyubchenko YL, Gall AA, Shlyakhtenko SL, Harrington RE (1992) Imaging DNA molecules chemically bound to a mica surface. In: **Scanning Probe Microscopies**, Manne S (ed.), Proc. SPIE **1639**, pp 84-89.

Matthews REF (1981) **Plant Virology**, Second Edition. Academic Press, New York, pp. 133, 723.

Neuberger A, Tatum EL (1975) **Frontiers of Biology, Vol. 39**. American Elsevier Publishing Co., New York, p. 23.
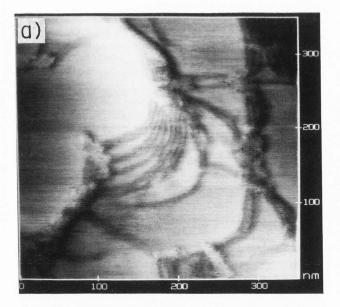
Oden PI, Nagahara LA, Graham JJ, Pan J, Tao NJ, Li Y, Thundat T, DeRose JA, Lindsay SM (1992) Atomic force and scanning tunneling microscopy observations of whisker crystals and surface modification on evaporated gold films. Ultramicrosc. **42-44**: 580-586.
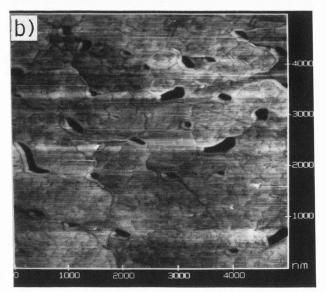
Sarid D (1991) **Atomic Force Microscopy**. Oxford University Press, New York, Chapter 13.

Thundat T, Allison DP, Warmack RJ, Ferrell TL (1992a) Imaging isolated strands of DNA molecules by atomic force microscopy. Ultramicrosc. **42-44**: 1101-1106.

Thundat T, Warmack RJ, Allison DP, Bottomley LA, Lourenco AJ, Ferrell TL (1992b) Atomic force microscopy of deoxyribonucleic acid strands adsorbed on mica: The effect of humidity on apparent width and image contrast. J. Vac. Sci. Technol. **A10**: 630-635.

Figure 7. AFM images of evaporated gold on mica. (a) 350 nm X 350 nm scan taken with a sharp tip showing atomic steps. Black (low) to white (high) corresponds to 36 nm. (b) 5000 nm X 5000 nm scan taken with a sharp tip showing details that are not seen when imaged with a normal tip (c). Black (low) to white (high) corresponds to 176 nm and 377 nm for (b) and (c), respectively.

Discussion with Reviewers

R. Balhorn: The value calculated for the radius of curvature of the conventional tip is much lower (10.9 versus 30-50 nm) than that reported by others. Our own experiences with these tips suggest that the best of these tips have a radius of curvature of 20 nm, almost twice the value calculated by this approach. Please comment.

Authors: We agree that the tip radius calculated by this method is smaller than that reported in the literature. This represents an upper limit since we used the full width at the substrate surface. One possible explanation for increased width of biomolecules observed by many experimenters is the lack of humidity control. We have systematically shown this fact in a recent paper (Thundat *et al.*, 1992b).

J.K.H. Hörber: How can the authors fill into their picture of possible resolution in AFM at the present time, the reported high resolution (in x and y) on very small objects like single fatty acid molecules in a Langmuir-Blodgett film array that has been transferred from the air/water interface, e.g., onto mica prior to imaging with AFM?

Authors: The structural resolution that can be achieved by AFM depends on both the radius of the tip and the geometry of the sample. The effect of tip radius becomes less important with samples that are less corrugated. For strongly corrugated samples the broadening

Thundat T, Allison DP, Warmack RJ, Brown G, Jacobson KB, Ferrell TL (1992c) Atomic force microscopy of DNA adsorbed on mica and modified mica. Scanning Microscopy **6**: 911-918.

Vesenka J, Guthold M, Tang CL, Keller D, Delaine E, Bustamante C (1992) A substrate preparation for reliable imaging of DNA molecules with scanning force microscope. Ultramicrosc. **42-44**: 1243-1249.

Wolter O, Bayer Th, Greschner J (1991) Micromachined silicon sensors for atomic force microscope. J. Vac. Sci. Technol. **B9**: 1353-1357.
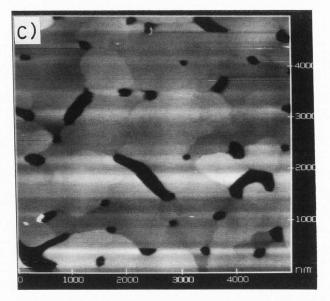
is strongly dependent on tip radius. Flat samples with very small periodic structures are thought to imaged by a unique tip asperity.

J.K.H. Hörber: Would the authors, based upon their experience with AFM tips, suggest that almost everything in terms of atomic or molecular resolution we have seen in AFM imaging is based on a periodic type array imaging rather than real imaging of single objects in real space with all its details like defects, grain boundaries and so on, which should be imaged in a "true picture."
Authors: We do not believe that only periodic arrays can be imaged at high resolution with AFM. We have found reproducible atomic defects in some AFM images of inorganic crystals (T. Thundat *et al.*, to be published).

J.K.H. Hörber: Is there a limit of the tips getting sharp in terms of the pressure getting too high for non-destructive imaging of soft biomolecules?
Authors: We do believe that there is a limit above which the AFM tip can rip biomolecules apart due to increased pressure. For example, DNA and TMV tended to break when we increased the force by few nNs. The sharper tips break the DNA strands at lower forces than blunt tips. A counterbalancing effect of sharper tips, however, is that the capillary force is reduced.

J.K.H. Hörber: Do these very fine tips break during the first contact with the sample?
Authors: As the sample approaches the tip, at some distance the tip jumps to the sample surface. We speculate that this abrupt jumping of the tip may destroy its sharp apex. We do see changes in DNA widths during scanning. We attribute this to tip picking up or losing small particles or clusters of molecules during scanning. Following scanning, electron-beam sharpened tips often show broken ends.

J.K.H. Hörber: I think it is important to note that the AFM image of atomic step on gold (Fig. 7a) do not show atomic resolution in x and y. We have studied this problem in detail by investigating monatomic steps on substrate crystals and never could resolve atomically the boundary in x and y but always in z (J. Schneider, W.M. Heckl, Scanning Probe Microscopies and Organics, Conference held in Martinsried, Munchen 1992, to be published).
Authors: We have observed atomic resolution on gold routinely by AFM when small areas (10 nm X 10 nm) are scanned. However, those images do not show any steps. Whenever atomic steps are observed no atomic resolution could be achieved. The image shown in Fig. 7a is too large to show atomic resolution.

Reviewer III: It appears that the "width" means the width at the base of the topographic trace across the test structure. It is misleading to compare this to the actual width of the molecules and conclude that the apparent width is larger, since it must be so. A more reasonable way to extract a width from the topographic trace would probably be FWHM, or full width at half maximum of the trace.
Authors: The apparent width of the sample should be measured at the base and not at FWHM. It is the width at the base that represents the total width of the contacting surfaces of the sample and the tip. Moreover, the envelope is not a gaussian and therefore FWHM has no meaning.